LA-10619-HDR, Part 3

UC-66b
Issued: December 1987

LA--10619-HDR-Pt.3

DE88 005086

Geological Structures from Televiewer Logs of GT-2, Fenton Hill, New Mexico

Part 3: Quality Control

Kerry L. Burns

Los Alamos National Laboratory
Los Alamos, New Mexico 87545

DISCLAIMER

CONTENTS

GEOLOGICAL STRUCTURES FROM TELEVIEWER LOGS OF GT-2, FENTON HILL, NEW MEXICO

Part 3: Quality Control

by

Kerry L. Burns

ABSTRACT

A procedure has been developed for extracting geological structures from paper prints of intensity-mode televiewer logs. It was applied to old logs of drill hole GT-2 at the Fenton Hill, New Mexico, Hot Dry Rock Site. A series of tests have also been developed for measuring the resultant data quality, and this report describes these tests and applies them to evaluate the procedure.

A test for measurement accuracy shows that locations were measured to better than 0.1 ft and orientations to within 1°. The root-mean-square error in fitting a trace rarely exceeded 0.2 ft. When the threshold for this error was set at 0.5911 ft, the pattern discriminator accepted 50% of the traces submitted to it. The probability that any trace would be accepted was 53.63%.

The second set of tests, for reproducibility, measures the amount of association between two different runs of the same length of hole, in this case a distance of 275 ft. Two new measures of association are defined, termed coplanarity and collinearity. The coplanarity measured about 60° at arbitrary lags, when the runs were not associated, falling to 43.5° at zero lag, when the runs were matched, demonstrating the existence of a genuine signal. However, no single feature recurs on both runs.

The lack of any recurrences requires explanation and leads to a third set of tests, for repetition rate. The low repetition rate is explained by random errors in location and orientation, which are different on each run. Location error is estimated at 14 ft for foliations and 8 ft for joints. This error is attributed to nonrepeated positioning in depth, off-centering, and tilting. The orientation error is

estimated at 10° for both foliations and joints. This error is attributed to nonrepeated motions such as drag, bounce, and oscillations of the logging tool. The amount of error shows that tool design must be improved to reduce mechanical suspension effects.

A fourth set of tests consists of fitting a model of the feature-extraction process to the data and estimating data reliability from quality parameters of the model. A perception model yielded an estimate of data quality at 91.5%. Because the estimate exceeds 90%, the data quality is considered acceptable and the feature-extraction system successful. However, the rate of feature extraction, estimated at 26.5% for foliations and 11.3% for joints, is only a fraction of that for recovered core and represents a significant loss of information. The positive perception probability of 27.0% for foliations and 11.5% for joints is about half that for high-quality photographic imagery, showing that digital recording and playback at advanced image-processing facilities would improve the results significantly.

I. INTRODUCTION

Scope of This Report

A method of extracting structural data from televiewer imagery has been developed, using as trial data some extremely poor imagery from drill hole GT-2 at Fenton Hill. Part 1 of this report described pattern recognition and pattern discrimination; Part 2, rectification to geographic coordinates. This part describes quality control methods. Interpretative processing for geomechanical parameters is another matter altogether.

II. QUALITY CONTROL MEASUREMENTS

A. Measurement Accuracy

Table I shows the results of repeated measurements of a strong joint, made at widely separated times over a period of weeks. The standard deviations indicate probable measurement error. The tabulation shows that orientations were measured to better than 1° and locations to better than 0.1 ft.

B. Fit to Prescribed Functional Form

Structural traces were selected according to their match to a specific functional form. A match was defined if the root-mean-square (rms) deviation,

TABLE I: MEASUREMENT ACCURACY, ESTIMATED FROM REPETITIVE MEASUREMENTS OF A STRONG JOINT (The results in the table show that orientations are measured to better than 1° and locations to better than 0.1 ft.)

	Orientation		Location		
Depth (ft)	Azimuth (deg)	Inclination (deg)	North (ft)	East (ft)	Down (ft)
2594.86	12.17	13.76	-1732.71	-1545.04	2599.41
2594.84	13.04	13.48	-1732.71	-1545.04	2599.39
2594.79	13.02	13.84	-1732.71	-1545.04	2599.34
2594.95	11.9	14.25	-1732.71	-1545.05	2599.50
2594.95	12.74	14.65	-1732.71	-1545.05	2599.50
2594.93	11.43	14.64	-1732.71	-1545.04	2599.48
2594.93	11.2	13.91	-1732.71	-1545.04	2599.48
standard deviations --					
0.0582	0.6290	0.4168	0.0000	0.0045	0.0582

between the actual trace and the best-fit form, was less than a prescribed threshold. The threshold that causes 50% of the tests to be declared matches is termed the 50% discriminant. If y is an altitude on the image for a given azimuth, and if y' is the altitude given by a least-squares fit to the trace, the rms error in fitting the trace is e_2, where

$$e_2 = [(1/K)S\{e_1^2(k)\}]^{1/2}; \quad e_1(k) = y_k - y'_k \quad .$$

The term S{} means summation over k from 1 to K, k is a point on the trace, and K is the number of points on the trace (usually about 20). Figure 1 shows e_2 for several hundred accepted traces. The rms error in fitting a trace rarely exceeded 0.2 ft.

C. Discriminator Acceptance Rate

The acceptance statistic, e_3, was computed as

$$e_3 = [(1/J)S\{T\{e^2(k)\}\}]^{1/2} \quad ,$$

where J is the number of traces in the set, S{} is summation over j from 1 to J, and T{} is summation over k from 1 to K. Figure 2 shows histograms of e_3 for J = 1322. The discriminant at the 50% level is 0.59 ft. The interpreter submitted 1322 traces to the pattern discriminator, which accepted 709. This is an acceptance probability of U = 709/1322 = 0.54 and a rejection probability of (1 - U) = 0.46.

III. REPRODUCIBILITY

A. Introduction

Reproducibility is a coefficient of association between data sets obtained on different runs of the data acquisition subsystem. Short segments of televiewer runs 1 and 2 overlapped, between about 4000 and 4275 ft downhole, and the overlapping enabled a test for reproducibility.

For real-valued variables, an appropriate coefficient is either correlation or covariance. A multistate coefficient designed for testing the output of perception systems was defined by Burns, Shepherd, and Berman 1977. In this case, neither is appropriate, so we introduce two new coefficients named "coplanarity" and "collinearity."

B. Definition of Coplanarity

The coplanarity, P, is defined by

$$P_{12} = 1 - E\{(\underline{a}_j \cdot \underline{b}_i \times \underline{b}_k)/|\underline{b}_i \times \underline{b}_k|;\ i+1=k;$$

$$d(\underline{b}_i) < m+d(\underline{a}_j) < d(\underline{b}_k);\ i=1,B-1;\ j=1,A\}$$

and

$$P_{21} = 1 - E\{(\underline{b}_j \cdot \underline{a}_i \times \underline{a}_k)/|\underline{a}_i \times \underline{a}_k|;\ i+1=k;$$

$$m+d(\underline{a}_i) < d(\underline{b}_j) < m+d(\underline{a}_k);\ i=1,A-1;\ j=1,B\} \quad ,$$

The orientation vectors observed in run 1 are $\{\underline{a}_i;\ i=1,A\}$, and those observed in run 2 are $\{\underline{b}_i;\ i=1,3\}$. The operators x and • are vector and scalar

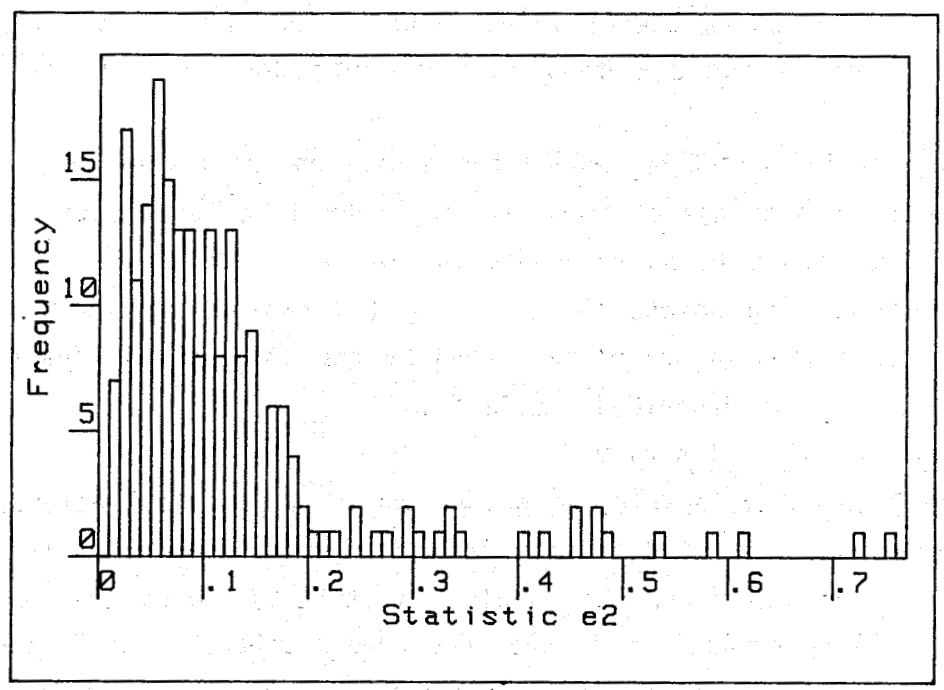

Figure 1. Fitting error. Histogram of statistic e_2 for run 1, from 4000 to 4545 ft depth. The histogram shows that the error in fitting a trace rarely exceeded 0.2 ft.

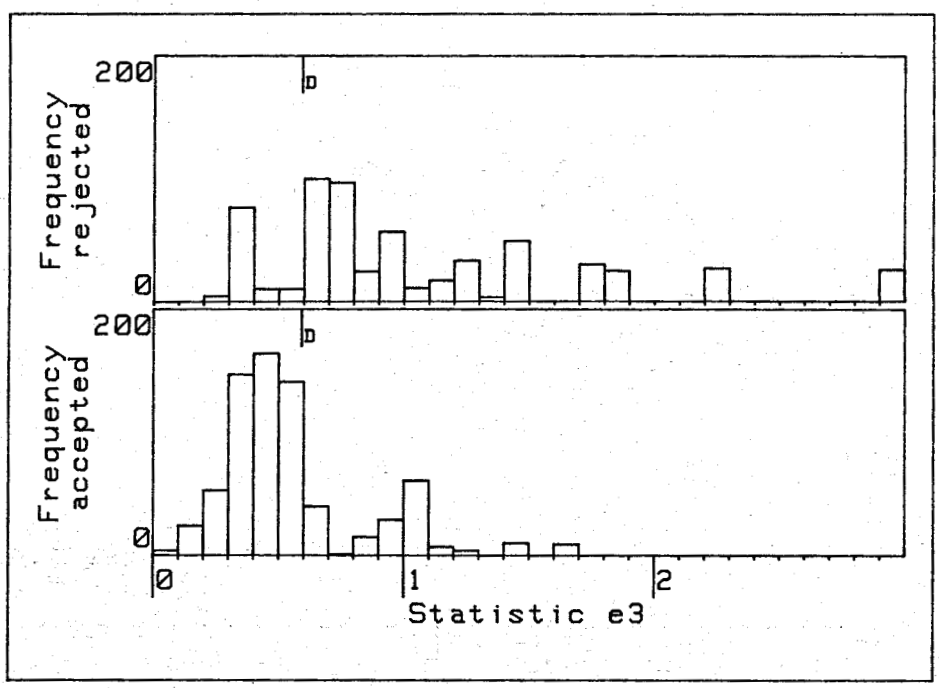

Figure 2. Recognition error. Histogram of statistic e_3 for runs 1 and 2, 2536 to 4545 ft depth. The top diagram is of rejected traces; the bottom is of accepted traces. The discriminant at the 50% level is 0.59 ft (marked "D").

products. |s| indicates the unsigned value of the scalar s. m is the lag (run 1 + lag versus run 2); d(a) is the depth downhole of the structure oriented a.

The measure P_{12} might be termed the cross-coplanarity of run 1 given run 2. It is a measure of association, varying from 0 (no association, the first orientation from run 1 being perpendicular to the plane formed by the orientations of neighboring points in run 2) to 1 (complete agreement, where the vector from run 1 lies in the plane formed by the two vectors from run 2). The other measure, P_{12}, is described similarly.

C. Observations of Coplanarity

Figure 3 shows coplanarity as a function of lag for foliations. The coplanarity measures angular deviation from a plane. The angle is INVCOS(P). From Figure 3 and Table II, this angle was about 60° when the runs are not associated, falling to 43.5° when the runs were matched. This is well-defined maximum, so the foliations are reproducible between the two televiewer runs.

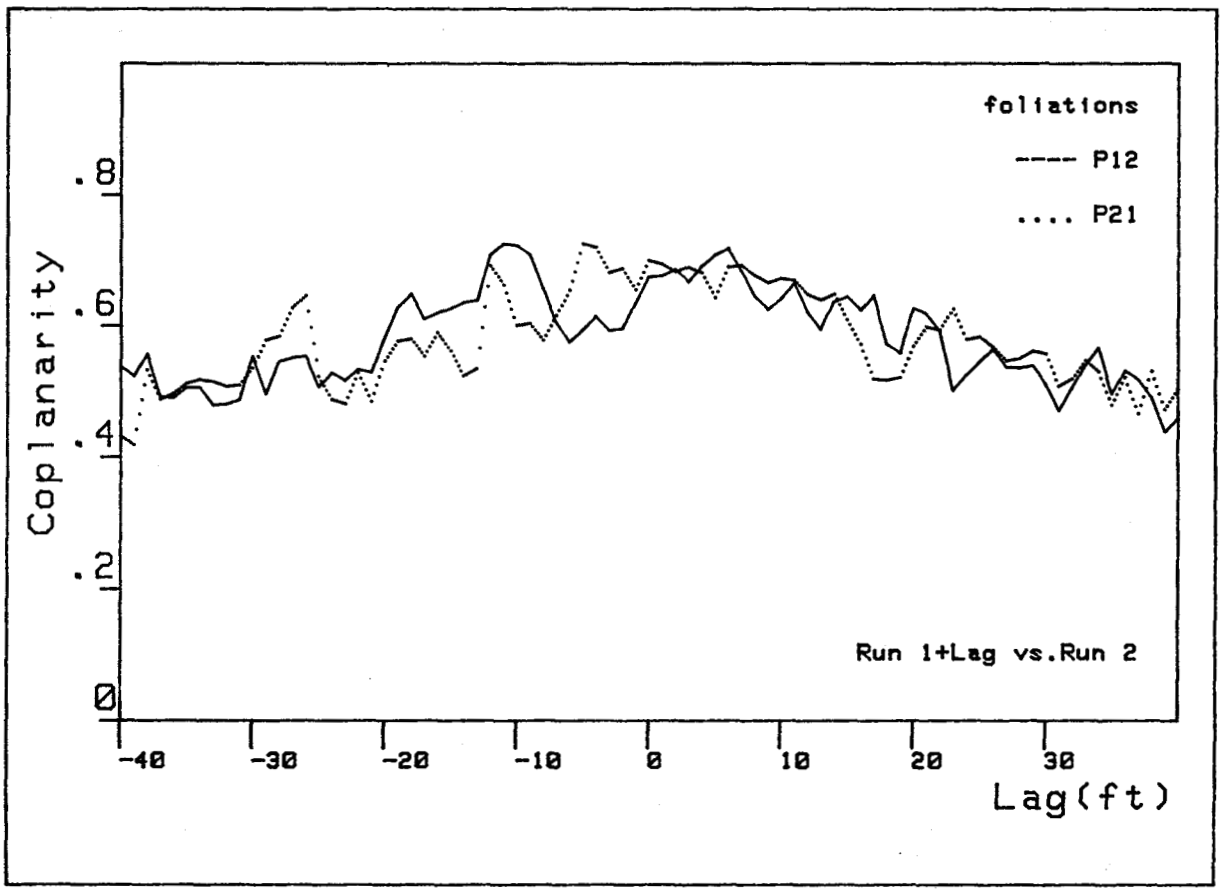

Figure 3. Coplanarity of foliations for run 1 + lag versus run 2, 4000 to 4275 ft depth. The plot indicates that the best match is at a lag of -4.5 ft.

TABLE II: REPRODUCIBILITY
(Run 1 + lag versus run 2, 4000-4275 ft depth)

Name of Statistic	Coefficient (range 0 - 1)	Lag (range -20 to 20 ft)
Foliation Coplanarity (Figure 3)		
mode in P	0.7253	-11.
mode in P (max)	0.7258	- 5.
mode in P	0.7006	0.
weighted mean		+ 0.02
mode in P	0.7185	+ 6.
	---	
mean P	0.6353	
st.dev.P	0.0539	
Foliation Collinearity (Figure 5)		
mode in L	0.8408	-11.
mode in L	0.8140	-11.
mode in L	0.8402	- 7.
mode in L (max)	0.8873	- 4.
mode in L	0.8776	0.
weighted mean		+ 0.01
mode in L	0.8528	+ 3.
mode in L	0.8323	+ 6.
mode in L	0.8745	+ 7.
	---	
mean L	0.8004	
st.dev.L	0.0358	
Fracture Coplanarity (Figure 4)		
mode in P (max)	0.7263	-15.
mode in P	0.6386	-11.
weighted mean		- 0.32
mode in P	0.6419	0.
mode in P	0.6626	+10.
	---	
mean P	0.5905	
st.dev.P	0.0480	

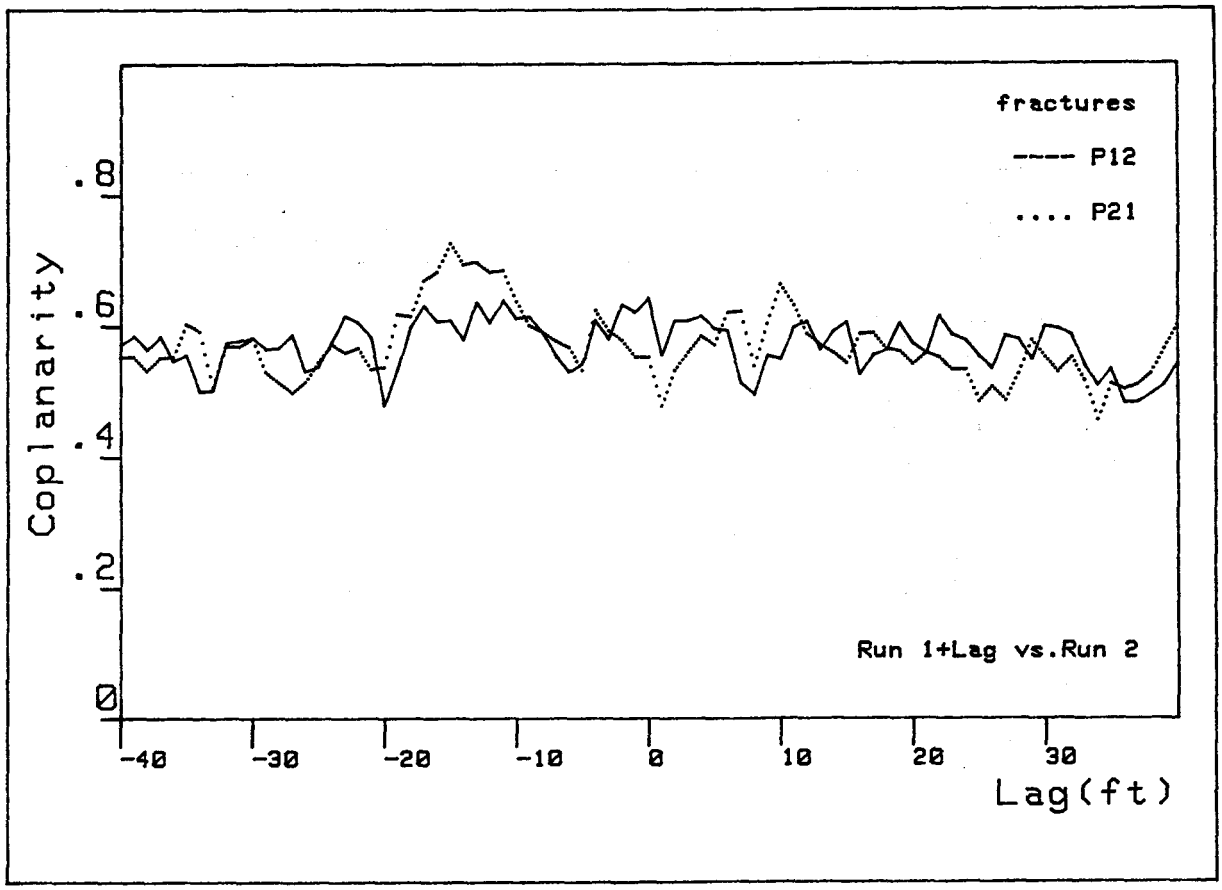

Figure 4. Coplanarity of fractures for run 1 + lag versus run 2, 4000 to 4269 ft depth. The lack of a systematic maximum indicates no serial correlation.

Figure 4 shows coplanarity versus lag for fractures. There was no systematic maximum, so the fractures are not reproducible between the two televiewer runs. The results for foliations and fractures are different because the foliations are serially correlated, while fractures are not, as is usually the case. If televiewer runs are to be correlated in the stratigraphic sense (that is, matched) by this method, it is necessary to use foliations.

D. Definition of Collinearity

The probability of a low coplanarity decreases with increasing angular separation of the two reference vectors. We may allow for that effect by multiplying by the vector area formed by the reference vectors. The result is the coefficient termed collinearity, L, which is defined by

$$L_{12} = 1 - E\{(\underline{a}_j \cdot \underline{b}_i \times \underline{b}_k);\ i+1=k;$$

$$d(\underline{b}_i) < d(\underline{a}_j) < d(\underline{b}_k);\ i=1,B-1;\ j=1,A\}$$

$$L_{21} = 1 - E\{(\underline{b}_j \cdot \underline{a}_i \times \underline{a}_k);\ i+1=k;$$

$$m+d(\underline{a}_i) < d(\underline{b}_j) < m+d(\underline{a}_k);\ i=1,A-1;\ j=1,B\} \quad .$$

E. Observations of Collinearity

Figure 5 shows collinearity as a function of lag for foliations. The result is similar to Figure 3. The periodicity in the difference $(L_{12}-L_{21})$ is interpreted as due to folds in the foliation, with a wavelength (if the folds were symmetrical) of 80 ft.

The match between the two runs was not well defined. Possible matching points are listed in Table II. One choice was at a lag of -4.5 ft, that is, a systematic error of 4.5 ft in the footage between the two runs. This error could easily have arisen with manual methods of operating the recorder.

IV. REPETITION RATE

A. Definition

No individual structure could be matched between the two runs within the limits of measurement error. However, if there was some fuzziness in location and orientation, the number of repetitions between the runs could be determined as N, where

$$N(z,r) = |\{|\underline{x}_i - \underline{y}_j| < z;\ \underline{p}_i \cdot \underline{q}_j > \cos(r);\ i=1,A;\ j=1,B\}|$$

with two conditions

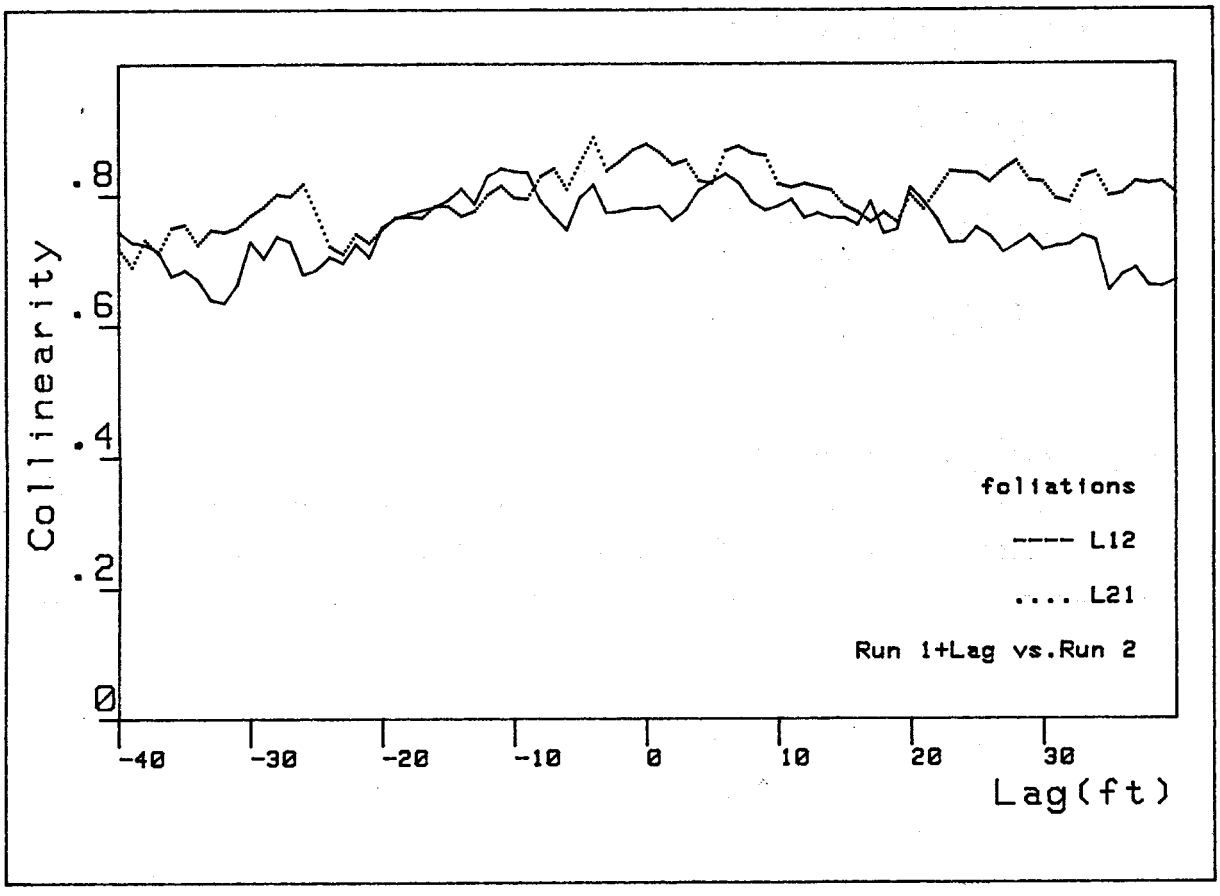

Figure 5. Collinearity of foliations for run 1 + lag versus run 2, 4000 to 4275 ft depth. The periodicity in the difference L_{12}-L_{21} indicates the presence of folds with a wavelength of about 80 ft.

$$|\{|\underline{x}_i - \underline{y}_j| < z;\ \underline{p}_i \cdot \underline{q}_j > \cos(r);\ j=1,B\}| <= 1 \text{ for } i=1,A$$

and

$$|\{|\underline{x}_i - \underline{y}_j| < z;\ \underline{p}_i \cdot \underline{q}_j > \cos(r);\ i=1,A\}| <= 1 \text{ for } j=1,B \quad .$$

In this expression $\underline{x}_i$ is the location and $\underline{p}_i$ the orientation of a structure from run 1; $\underline{y}_j$ is the location and $\underline{q}_j$ the orientation of a structure from run 2; A and B are the numbers of structures in the region of overlap between runs 1 and 2; and z and r are the fuzziness in location and orientation, respectively.

B. Observations of Repetition Rate

Figure 6 shows N for foliations, as a function of z and r. Limiting values are denoted by the periods and are values of z or r above which one of the two conditions failed. The optimum estimate of the number of repetitions was obtained by maximizing N(z,r) while minimizing z and r. For foliations (Figure 6) the number was 5 at z = 14 ft and r = 10°. For joints (Figure 7) the number of repetitions was 5 at z = 8 ft and r = 10°.

The fuzziness was larger than the measurement accuracy determined in Section II.A above, indicating the existence of a random process in parameter estimation that is independent of the random decision process in feature extraction.

V. PERCEPTION MODEL

A. General Description

To assess data quality required formulating a model of the information processing scheme shown in Part 1 (Figure 11). The system was a sequence of operations, each of which had a specific effect on the information transmitted. Two separate random processes were involved, one arising in the instrumental system that generated the imagery, the other in the feature-extraction system that obtained information from the imagery. Feature extraction involved human annotation (interrupt no. K5 in Figure 11, Part 1), so the model had to take into account human decision-making processes at that step. Norbert Weiner demonstrated, during World War II, that human reaction times must be incorporated into the design of weapons systems. Here the model had to incorporate, not human reaction times, but the human decision-making capability. Methods of dealing with human decisions were developed under the auspices of NASA by Burns and Brown in 1977, following work on psycho-perception by Westinghouse. The characteristic of human decision-making systems is that they involve, not only the "positive" signals and noise of instrumental systems, but also "negative" signals and noise, as explained below, so that the monomial stochastic variables of ordinary instrumental systems have to be generalized to multinomial.

B. Definition of Perception Model

A simple 2 x 2 perception model is illustrated in Table III. The imagery contains structural traces or vector trends (features of type 1) and image

angle (deg)	footage (ft) 1	2	3	4	5	6	7	8	9	10	12	13	14	15	16	18	22	23	24	40	57	60
1	0	0	0	0	0	0	0	0	0	0	0	0	0	0	0	0	0	0	0	0	0	0
2	0	0	0	0	0	0	0	0	0	0	0	0	0	0	0	0	0	0	0	0	0	0
3	0	0	0	0	0	0	0	0	0	0	0	0	0	0	0	1	1	1	1	1	1	1
4	0	0	0	0	0	0	0	0	0	0	0	0	0	0	0	1	1	1	1	1	1	1
5	0	0	0	0	0	0	0	0	0	0	0	0	0	0	0	1	1	1	1	1	1	1
6	0	0	0	0	0	0	0	0	0	0	0	0	0	1	1	2	2	2	2.	2.	3.	3.
7	0	0	0	0	0	0	1	1	1	1	1	2	2	3.	3.	4.	4.	5.				
8	0	0	0	1	1	1	2	2	2	2	2	3	3.									
10	0	0	0	1	1	3	4.	4.	4.	4.	4.	5.	5.									
11	0	0	0	1	2.	4.																
12	0	0	0	1.																		
15	0	0	0.	1.																		
16	1	1.																				
20	1	1.																				
22	1	2.																				
23	1	2.																				
24	2.																					
29	2.																					
30	3.																					
32	REPETITION OF FOLIATIONS																					

Figure 6. Repetition of foliations. The figure contains the number of foliations that are closer together in depth than the footage and closer together in orientation than the angle. Limiting values are denoted by the periods. The optimum is defined as the maximum in the limiting set with smallest footage and angle. The optimum is observed to be five foliations at 14 ft and 10°.

angle (deg)	footage (ft) 1	2	3	4	5	6	7	8	9	10	12	14	16	22	24	27	28	32	33	34	35	49	50	60
1	0	0	0	0	0	0	0	0	0	0	0	0	0	0	0	0	0	0	0	0	0	0	0	0
2	0	0	0	0	0	0	0	0	0	1	1	1	1	1	1	1	1	1	1	1	1	1	1	1
3	0	0	0	0	0	1	1	1	1	2	2	2	3	3	3	3	3	3	3	3	3	3	4	4
4	0	0	0	0	0	1	1	1	1	2	2	2	3	3	3	3	3	3	4	4	4.	4.	5.	5.
5	0	0	0	0	0	1	1	2	2	3	3	4	5	5	5	5	5.	5.	5.	5.				
6	1	1	1	1	1	2	2	3	3	4	5	6	7	7	8	8.								
7	1	1	1	1	1	2	2	3	3	4	5	6	8	8	9	9.								
8	1	1	1	1	1	2	2	3	3.	4.	5.	6.	8.	8.	9.	9.								
9	1	1	1	1	1	2	3	5.																
10	1	1	1	1.	1.	2.	3.	5.																
11	1	1	1.																					
12	1	2	3.																					
17	1	2	3.																					
18	2.	3.	4.																					
19	REPETITION OF JOINTS																							

Figure 7. Repetition of joints. Description as for Figure 6. The optimum was observed to be five joints at 8 ft and 10°.

TABLE III: DIAGRAM OF A SIMPLE 2 x 2 PERCEPTION MODEL WITH TWO TYPES OF FEATURES (structure and artifact) AND TWO LEVELS OF RECOGNITION (seen and not seen) (Based on Burns and Brown 1978)

Feature Extracted	Feature on Image	
Feature--	Structure	Artifact
proportion	$(1-\alpha)$	α
quantity	$A_1=S\beta(1-\alpha)$	$A_0=S\beta\alpha$
Structure--		
probability	H_1	$1-H_0$
quantity	$A_{11}=S\beta(1-\alpha)H_1$	$A_{01}=S\beta\alpha(1-H_0)$
(name)	(truly seen)	(falsely seen)
Artifact--		
probability	$1-H_1$	H_0
quantity	$A_{10}=S\beta(1-\alpha)(1-H_1)$	$A_{00}=S\beta\alpha H_0$
(name)	(falsely omitted)	(truly omitted)

artifacts (features of type 0). If S is a length of wellbore, let $S\beta$ be the number of features so that β is the spatial frequency (number per foot) of features of either type. Let α be the proportion of artifacts so that the number of artifacts is $S\beta\alpha$, while the number of structures is $S\beta(1-\alpha)$. Let H be the probability of recognizing an artifact as an artifact, that is, not annotating the feature; then $1-P_0$ is the probability of annotating an artifact as if it were a structure. Let P_1 be the probability of recognizing a structure as a structure; then $1-P_1$ is the probability of thinking the artifact is a structure and not annotating it.

If there are k repeated inspections, the number of structures that will be repeated on r of those inspections is N, where, according to the binomial "model A" of Burns and Brown 1978,

$$N = S\beta C(k,r)\{\alpha P_0^{k-r}(1-P_0)^r + (1-\alpha)(1-P_1)^{k-r}P_1^r\} \quad , \qquad (1)$$

where $C(k,r) = n!/(r!(n-r)!)$ is the number of combinations of k things, r at a time, and since $0!=1$, $C(k,r)=1$ if $k=r$.

C. Fitting the Perception Model to Observations

On examination of C_s (19.605 ft) of core, Laughlin et al. (1983) found C_n (8 foliations, 34 joints). An appropriate model is $k=1$, $r=1$, $P_0=1$, $P_1=1$ so that Equation (1) becomes:

$$C_s\beta(1-\alpha) = C_n \quad . \tag{2}$$

The first stage in televiewer information extraction was human selection and annotation (step 11 of Figure 11, Part 1) followed by a computer test of goodness of fit (step 13 of Figure 11, Part 1). If the combined result was R_n structures from R_s feet of televiewer imagery, then an appropriate model for step 11 is $k=1$, $r=1$ so that Equation (1) becomes

$$R_s\beta\{\alpha(1-H_0) + (1-\alpha)H_1\}\cdot U = R_n \quad , \tag{3}$$

where H_0 and H_1 are the human perception probabilities in step 11 and U is the acceptance rate of step 13.

Step 13 is pattern discrimination. Let X_1 be the probability that an annotated structure was accepted by the pattern discriminator, and let X_0 be the probability that an artifact was rejected. An appropriate model for step 13 is $k=1$, $r=1$ so that Equation (1) becomes

$$R_s\beta\{\alpha(1-H_0)(1-X_0) + (1-\alpha)H_1X_1\} = R_n \quad . \tag{4}$$

Equations (2), (3), and (4) are soluble for H_1 and together constitute a system that will be termed "model A." Applying model A yielded the results in Table IV. The pattern discriminator was a chi-square test at the 90% confidence level, so it was assumed that $X_0 = X_1 = 0.9000$. The results in Table IV

TABLE IV: DATA QUALITY

Measure	Foliations	Joints
After annotation:		
R_s	2294.73	-11.
R_n	248.	- 5.
H_1	0.2704	0.
$A_{01}(a)$	0.0491	+ 0.02
$A_1(a)$	0.0589	+ 6.
$Q_1(a)$	0.5454	
After pattern discrimination:		
H_1	0.2704	
$A_{01}(d)$	0.0092	
$A_{11}(d)$	0.0989	-11.
$Q_1(d)$	0.9152	-11.

From overlap between runs:

	run 1	run 2	run 1	run 2
R_s (ft)	266.9	266.9	266.9	266.9
R_n (no)	33.	40.	50.	52.
H_1	0.3094	0.3750	0.1103	0.1147
$A_{01}(a)$	0.0562	0.0681	0.0852	0.0886
$A_{11}(a)$	0.0674	0.0817	0.1022	0.1063
$Q_1(a)$	0.5454	0.5454	0.5454	0.5454
$A_{01}(d)$	0.0105	0.0127	0.0159	0.0165
$A_{11}(d)$	0.1132	0.1372	0.1715	0.1783
$Q_1(d)$	0.9152	0.9152	0.9152	0.9152
Expected L :				
if $H_0 = 0$	10.5		5.2	
if $H_0 = 0.5$	10.3		4.9	
if $H_0 = 1$	10.2		4.7	
L_n observed	14 (Figure 6)		5 (Figure 7)	

The results in Table IV represent solutions to the system:

(1) $C_s.\beta\{1-\alpha\} = C_n$;

(2) $R_s.\beta\{\alpha(1-H_0)+(1-\alpha)H_1\}.U = R_n$;

(3) $R_s.\beta\{\alpha(1-H_0)(1-X_0)+(1-\alpha)H_1.X_1\} = R_n$; and

(4) $L_s.\beta\{\alpha(1-H_{01})(1-X_0)(1-H_{02})(1-X_0) + (1-a)H_{11}.X_1.H_{12}.X_1\} = L_n$;

given that

(5) $C_s = 19.685$,

(6) $C_n = 8$ (foliations) or $C_n = 34$ (joints),

(7) $0 < H_0, H_1, \alpha < 1$,

(8) $U = 0.5363$,

(9) $X_0 = X_1 = 0.9$, and

(10) $\beta > C_n/C_s$.

show that H_1 was 0.2704 for foliations, 0.1149 for joints. That is, there was a 27.04% probability that a human would recognize a foliation as a foliation and annotate it.

The positive signal and noise are denoted A_{11} and A_{01}, respectively, where, following annotation (step 11 of Figure 11, Part 1),

$$A_{01}\ (a) = \alpha(1-H_0)$$

and

$$A_{11}\ (a) = (1-\alpha)H_1$$

and where, following pattern discrimination (step 13 of Figure 11, Part 1),

$$A_{01}\ (d) = \alpha(1-H_0)(1-X_0)$$

and

$$A_{11}\ (d) = (1-\alpha)H_1X_1 \quad .$$

The data quality, Q_1, is the probability that a feature accepted by the system as a structure is truly a structure. This is measured by

$$Q_1 = A_{11}/(A_{01}+A_{11}) \quad .$$

The results in Table IV show that the data quality was 54.54% after annotation, while application of the pattern discriminator raised the quality to 91.52%. These results mean that the data meet a 90% experimental standard. The positive signal/noise ratio is A_{11}/A_{01} and is 10.75 for foliations and

10.83 for foliations, which exceed the experimental standard of 10. The structural data obtained by this procedure, as tabulated in Part 2, are therefore of acceptable quality.

VI. SUMMARY

Runs 1 and 2 overlap between 4000.97 and 4267.87 ft downhole. In that interval, 33 foliations and 50 fractures were found in run 1, while 40 foliations and 52 fractures were found in run 2. Applying model A yielded $H_1(d)$, $A_{01}(d)$, $A_{11}(d)$, and $Q_1(d)$ for each run separately, as shown in Table IV. There were small, unimportant differences in the runs.

A model A of the feature-extraction process yielded an estimate of data quality, Q_1, as 91.52%, which was an average for all 733 structures. Since Q_1 exceeded 90%, the data quality was acceptable provided the subsequent interpretation system could handle 8.48% of artifacts. A proportion of 8.48% "sports" or "outliers" is within the capacity of many statistical treatments, so to this extent, the feature-extraction system was successful.

The feature-extraction model indicated a positive perception probability of 27.04% (for foliations) and 11.49% (for joints). These amounts are about half those obtained with high-quality photographic imagery by Burns and Brown 1978. The reduction is attributed to electronic noise and poor recording quality. As a result, the feature extraction rate, estimated at 26.48% for foliations and 11.26% for joints, is only a fraction of that for recovered core. This significant loss of information could be virtually eliminated by digital recording and playback at advanced image-processing facilities.

Individual structures were not repeated between different runs of the same length of the wellbore, within measurement accuracy. However, the feature-extraction model predicted that 10 foliations and 5 joints would be repeated. To achieve a repetition rate near that predicted required introducing a fuzziness located at z ft and oriented at r°. The fuzziness was estimated at z = 14 ft, r = 10° for foliations, and z = 8 ft, r = 10° for joints. The fuzziness was attributed to a random process in the instrumental or operating system used to construct the imagery, that is, an instrumental error outside the feature-extraction method. The source of this instrumental error is in the location, centering, and motions of the tool.

The televiewer has considerable scope for improvement. By applying a pattern discriminator, we raised the quality of the output from 54.54% to 91.52%, but at the cost of a 46.37% loss of information. The addition of digital recording, playback, and image-processing would be expected to double the amount of information recovered, but only if there was no image distortion. Even with no distortion, 91.52% quality is about the same as that ordinarily yielded by high-quality photographic imagery, so we would not expect a significant improvement in output quality.

The fuzziness in estimated parameters of location and orientation was due to a random process outside the feature-extraction system and therefore would not be reduced by improvements in image quality. The instrument itself needs to be redesigned.

The interpretation methods required to deal with the data tabulated in Part 2 must be able to handle, not only the 8.48% of artifacts arising from the feature-extraction process, but also location errors (about 20 ft) and orientation errors (10°) arising from the instrument. Interpretation methods capable of handling the problem do exist, but they are necessarily statistical; methods that depend upon individuals will fail. Thus the data are unsuitable for such interpretative efforts as trying to project a single joint or fracture from one borehole to another.

REFERENCES

Burns, K.L., and G.H. Brown, 1978, "The Human Perception of Geological Lineaments and Other Discrete Features in Remote Sensing Immagery: Signal Strengths, Noise levels and Quality," Remote Sensing Environ., v. 7, n. 2, pp. 163-177.

Burns, K.L., J. Shepherd, and M. Berman, 1977, "Reproducibility of Geological Lineaments and Other Discrete Features Interpreted from Imagery: Measurement by a Coefficient of Association," Remote Sensing Environ., v. 5, n. 4, pp. 267-301.

Laughlin, A.W., A.C. Eddy, R. Laney, and M.J. Aldrich, 1983, Geology of the Fenton Hill, New Mexico, Hot Dry Rock Site," J. Volcanol. Geotherm. Res., v. 15, pp. 21-41